AD-752 229

QUASI-SINUSOIDAL GEOMAGNETIC VARIATIONS
AT GEOMAGNETIC MIDLATITUDE

John H. Frey, et al

Science Resources Foundation

Prepared for:

Air Force Cambridge Research Laboratories

31 July 1972

AFCRL - 72 - 0465

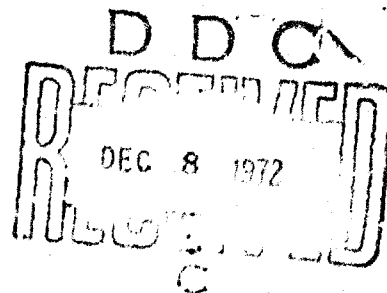## QUASI-SINUSOIDAL GEOMAGNETIC VARIATIONS
AT GEOMAGNETIC MIDLATITUDE

John H. Frey
William L. Fischer

Science Resources Foundation
50 Hunt Street
Watertown, Massachusetts 02172

Contract No. F19628-71-C-0178

Project No. 8601
Task No. 860107
Work Unit No. 86010701

D D C

DEC 8 1972

FINAL REPORT

Period Covered: 1 April 1971 through 30 June 1972

31 July 1972

Contract Monitor: Elwood Maple, Space Physics Laboratory

Approved for public release; distribution unlimited

Prepared
for

AIR FORCE CAMBRIDGE RESEARCH LABORATORIES
AIR FORCE SYSTEMS COMMAND
UNITED STATES AIR FORCE
BEDFORD, MASSACHUSETTS 01730

Qualified requestors may obtain additional copies from the
Defense Documentation Center. All others should apply to
the National Technical Information Service.

DOCUMENT CONTROL DATA - R & D

(Security classification of title, body of abstract and indexing annotation must be entered when the overall report is classified)

1 ORIGINATING ACTIVITY *(Corporate author)*	2a. REPORT SECURITY CLASSIFICATION
Science Resources Foundation 50 Hunt Street Watertown, Massachusetts 02172	UNCLASSIFIED
	2b GROUP

3 REPORT TITLE

QUASI-SINUSOIDAL GEOMAGNETIC VARIATIONS AT GEOMAGNETIC MIDLATITUDE

4 DESCRIPTIVE NOTES *(Type of report and inclusive dates)*

Scientific. Final. 1 April 1971 - 30 June 1972   Approved   7 September 1972

5 AUTHOR(S) *(First name, middle initial, last name)*

John H. Frey
William L. Fischer

6 REPORT DATE	7a TOTAL NO OF PAGES	7b NO OF REFS
31 July 1972	~~55~~ 60	11

8a. CONTRACT OR GRANT NO	9a ORIGINATOR'S REPORT NUMBER(S)
F19628-71-C-0178	
b PROJECT, TASK, AND WORK UNIT NO. 8601-07-01	
c. DOD ELEMENT 61102F	9b OTHER REPORT NO(S) *(Any other numbers that may be assigned this report)*
d. DOD SUBELEMENT 681311	AFCRL - 72 - 0465

10 DISTRIBUTION STATEMENT

Approved for public release; distribution unlimited.

11 SUPPLEMENTARY NOTES	12 SPONSORING MILITARY ACTIVITY
	Air Force Cambridge Research Laboratories (PH) L. G. Hanscom Field Bedford, Massachusetts 01730

13 ABSTRACT

Three-component quasi-sinusoidal geomagnetic variations (micropulsations) at Concord, Massachusetts for a five month period have been reduced to hourly average amplitudes in six contiguous octave frequency bands covering the period range from 16 to 1024 seconds. Original high and low sensitivity data have been merged to accommodate the 70 db dynamic range of the natural variations. The local time behavior and spectral characteristics of the variations are discussed. Results of various linear correlation analyses of the varying levels of magnetospheric excitation and to the origin and propagation of hydromagnetic waves in the period range covered are discussed.

DD FORM 1473

KEY WORDS	LINK A		LINK B		LINK C	
	ROLE	WT	ROLE	WT	ROLE	WT
average power spectral density (APSD)						
correlation coefficient						
diurnal variation						
geomagnetic disturbance						
geomagnetic variation						
hourly spectra						
hydromagnetic waves						
interplanetary magnetic field						
linear correlation						
local time variation						
magnetosphere						
mean absolute value (MAV)						
micropulsations						
M index						
occurrence frequency						
octave band						
persistence tendency						
quasi-sinusoidal variations						
recurrence tendency						
spectral enhancement						
stationarity						
superposed epoch						

AFCRL - 72 - 0465

QUASI-SINUSOIDAL GEOMAGNETIC VARIATIONS
AT GEOMAGNETIC MIDLATITUDE

John H. Frey
William L. Fischer

Science Resources Foundation
50 Hunt Street
Watertown, Massachusetts 02172

Contract No. F19628-71-C-0178

Project No. 8601
Task No. 860107
Work Unit No. 86010701

FINAL REPORT

Period Covered: 1 April 1971 through 30 June 1972

31 July 1972

Contract Monitor: Elwood Maple, Space Physics Laboratory

Prepared
for

III

TABLE OF CONTENTS

V

1. Introduction

The results presented in this report constitute the second phase of what has been a continuing study of the local time behavior of quasi-sinusoidal geomagnetic variations (micropulsations) at geomagnetic midlatitude and their relationship to varying levels of magnetospheric excitation.

The data selected for analysis were recorded at Concord, Massachusetts (approximate geomagnetic coordinates: $\phi = 54^\circ N, \Lambda = 0^\circ$. This location is favorable for observing geomagnetic micropulsations because it is on the prime geomagnetic meridian, i.e., local time and geomagnetic time are nearly coincident, and it is near the latitude of intersection of the quiet time plasma pause (Carpenter, 1966).

The geomagnetic sensors are induction coils in which the instaneously induced voltage is proportional to the time rate of change of the geomagnetic field. Three mutually perpendicular components: geographic north-south (X), geographic east-west (Y) and vertical (Z), are recorded. Each of the horizontal components has a high and low sensitivity channel to accommodate the 70 db dynamic range of the natural variations. Electromagnetic noise at power line frequency (60 Hz and its harmonics) propagates such that the natural vertical component is either obscured or highly contaminated except at times of high natural signal levels. A detailed discussion of instrumentation and system response is given by Frey (1969). [Results limited by termination of contract before the information available in the data which had been reduced could be fully exploited].

1

2. Primary Data Set

Approximately five months of geomagnetic data have been reduced to hourly average amplitudes in six contiguous octave frequency bands: T = 16-32, 32-64, 64-128, 128-256, 256-512, and 512-1024 **seconds**, respectively. Hourly estimates of the mean absolute value (MAV) of signal amplitude in γ and of the average power spectral density (APSD) in γ^2/mHz were obtained by successive stages of low-pass numerical (digital) filtering to minimize aliasing, of resampling and, finally, of spectral decomposition by numerical (digital) band-pass filtering. Detailed information concerning numerical filter design and data reduction procedures are given by Frey et al. (1970).

The time interval investigated was selected primarily on the basis of maximum continuity of data. It is also a subset of the much longer time interval for which a broad-band micropulsation index, M, data set has been generated. Octave band width hourly estimates of MAV and APSD were computed for 3185 hours representing 92.3% of the interval 11 April - 1 September 1967. Of the 141 days comprising this time interval, only 8 had 12 or more hours of data missing.

Although data was reduced for all three components, attention has been focused on analysis of the horizontal components because the noise contamination in the vertical component, mentioned previously, required special treatment and more time than was available.

For the sake of brevity, the six octave frequency bands are assigned code numbers as follows:

Period Band (Sec.)	Octave Designation
16-32	01
32-64	02
64-128	03
128-256	04
256-512	05
512-1024	06

They will be referred to by code number throughout the remainder of this report.

Considerable care was taken in preparing the octave band-width data files for subsequent analyses. Many of the computer programs outlined in Section 8 were created and implemented to insure the integrity of the data set. The conversion of the AFCRL Computations Center from the IBM 7094 DCS to the CDC 6600 computing system necessitated program and tape-file format modifications. A brief chronology of the salient phases of data processing is given below.

Initially the geomagnetic data set was contained on a punched card file but was incomplete. An existing IBM 7094 DCS program designed to obtain estimates of the APSD and the MAV for the six octave bands was modified for use on the CDC 6600 computer. Specifically, the convolution (numerical filtering) subroutine originally coded in the IBM 7094 assembly language, MAP, was replaced by a subroutine employing similar logic written in CDC FORTRAN IV. This modified program was then used to obtain APSD and MAV hourly estimates on punched cards for time intervals not contained in the original punched card file. Thus, the data set was made complete.

The card files punched by the numerical band-pass filtering
routine for the high and low sensitivity horizontal and the vertical
components were structured to provide successive pairs of card
images having six hours of data for the APSD and MAV, respectively.
From this card file, separate binary tape files were created, one
for the APSD hourly estimates and one for MAV hourly estimates.
Simultaneously with the creation of the binary tape files, data
editing was performed to check for mispunched and out-of-sequence
cards.

Times during which overloading occurred in the high sensitivity
horizontal components were ascertained by visual inspection of
oscillograph records prepared specifically for this purpose. Those
hours containing overloading were replaced by the corresponding low
sensitivity data adjusted for background noise.

3. Diurnal Behavior of Horizontal Component MAV's

The dominant characteristic of the local time behavior of micro-
pulsations is a strong diurnal variation in amplitude. Figures 1 and
2 illustrate this diurnal variation in the amplitude spectral estimates
for the X and Y components, respectively. The data are plotted for
each octave band by local hour and represent averages obtained when
18 days having a daily linear equivalent planetary amplitude index,
Ap, greater than 18 are excluded. To ascertain typical diurnal behavior,
it was necessary to exclude MAV estimates for these few unusually
disturbed days to remove the excessive bias and resulting distortion

4

introduced by them. Unfortunately, geomagnetically disturbed
intervals for this data set were too few in number and too poorly
distributed in time to permit an analysis of high disturbance
level effects on the diurnal behavior. The dynamic range of the
amplitude spectra (roughly .002 to .2 γ/mHz, in going from O1 to
O6) are representative of quiet to moderate levels of geomagnetic
activity.

The most interesting result displayed in Figures 1 and 2 is
the gross difference in diurnal behavior for X and Y. The X and
Y curves are similar in shape for O1, i.e., both have broad maxima
nearly symmetrical about local noon; but the curves become dis-
tinctly different with increasing period band, i.e., X has a maximum
after noon while a similarly shaped maximum in Y is displaced toward
the morning hours. For both components, the diurnal variation
becomes progressively weaker for the longer period octave bands.

The diurnal behavior patterns for the horizontal components
suggests that the major axes of elliptically polarized hydromagnetic
waves tend to lie in the east-west direction in the morning and in
the north-south direction in the afternoon. Moreover, this tendency
becomes more pronounced as wave periods increase. The similar
diurnal behavior of O1 spectral estimates for both X and Y indicates
a common energy source which probably lies in the interaction
between the solar wind flow and the magnetosphere at the sunward
magnetopause. The significance of the divergence between X and Y
diurnal behavior for longer period bands with respect to hydro-
magnetic wave excitation mechanisms will require more wr⋅ before

it can be elucidated.

4. Linear Product-Moment Correlation Analyses

Linear correlation analysis is a rather hazardous enterprise
because correlation coefficients are frequently misleading unless
accompanied by appropriate scatter plots which reveal their signifi-
cance. A few data points having relatively slight dispersion which
are widely separated from the majority of points (whatever their
dispersion) in a correlation between two parameters invariably result
in a high linear correlation coefficient which does not represent the
true relationship between those parameters. It was, of course,
impossible to obtain scatter plots for all of the numerous correlations
performed in this investigation. However, enough plots were obtained
to expose the pit-falls in the various correlation analyses described
below. The 3-hour linear equivalent planetary amplitude index, ap, is
used as an indication of the level of geomagnetic disturbance in
several of the correlation analyses.

A. Correlation Between Horizontal Component MAV's

Correlation between X-MAV and Y-MAV geomagnetic variation
amplitudes was performed by octave band for the total data set (for
all ap) and for ap > 48 excluded. The latter was done to eliminate
the few very large values which, regardless of their distribution
between X and Y, might contaminate the correlation. Table 1 gives
the correlation coefficients for both conditions by octave band. The

coefficients with all ap included are very high. The coefficients with ap > 48 excluded are relatively high for shorter period bands but decrease with increasing period band. Moreover, the correlation for respective octave bands are lower for ap > 48 excluded. It may also be observed that the difference between respective octave band coefficients increases significantly with increasing period band. These observations indicate that the few large values, in fact, do dominate the correlation when included and suggest that there is less uniform energy distribution between X and Y, especially for longer periods, when enhanced geomagnetic disturbance is excluded. Recall the progressively divergent behavior of X and Y with increasing period band noted in the previous section.

Correlations between X and Y MAV's by octave band with and without ap > 48 excluded were also performed for each local hour. The hourly correlations for both ap conditions are significantly high (r : 0.500) with the set having ap > 48 excluded being generally lower. The variations in correlation are relatively large and quite irregular. They exhibit no coherent time dependence and do not correspond well in detail from one octave band to another for either ap condition. The hourly coefficient sets tend toward lower correlation and greater difference in correlation between sets with increasing period band as does the correlation for the total data set.

A much longer data sample containing more intervals of enhanced geomagnetic activity would almost certainly result in correlation coefficients of greater physical significance but would not alter the fact that the average amplitude behavior of the horizontal components

7

correspond reasonably well in all octave bands.

B. Correlation Between M and Horizontal Component MAV's

A one hour, quasi-logarithmic index, M, has been used to characterize geomagnetic micropulsation activity levels by Frey et al. (1971). Micropulsation activity for the time interval considered here has been characterized in like manner except that the M index has been expanded to include a sixth category for extremely high activity. M is 99% derived from the X component. The distribution of M values for all hours of this data set is shown in Figure 3 in the six categories. The time interval was rather quiet as indicated by the preponderance of low M values, M = 1 and M = 2.

The nominal period range for M is 20 - 300 seconds, but activity having periods considerably less than 20 seconds is included when it is of sufficiently large amplitude, i.e., large pearl type pulsations and asymmetrical spikes due to local lightning. An attempt was made to exclude the obvious lightning contamination; unfortunately, all was not obvious. The period range for MAV's as previously indicated, is strictly 16 - 1024 seconds in six discrete octave bands. Time did not permit the preparation of three shorter period octave bands from 2 - 16 seconds which had been reduced from primary data sets.

The reason for correlating each discrete octave band with broad band M was to ascertain whether or not M had any generally preferred or time dependent period content. Of course, poor correlation implicitly indicates different frequency content for these parameters.

8

No scatter plots were made for this correlation analysis and no correlation of data with ap > 48 excluded was performed.

Linear correlations between M and each of the six octave band MAV's for X and Y amplitudes by total data set and by local hour were computed. The coefficients for the total data set are given by octave band in Table 1. Correlation between M and X - MAV is relatively low for all octave bands indicating a complex relationship between them. There is no clearly preferred period band contribution to M indicated. Rather, there is a progressive (except for O5) decrease in correlation with longer period bands probably due to the combined effects of the ample shorter period content of M and the intentional de-emphasis of its longer period content (equivalent to O5 and C6). Correlation between M and Y - MAV is slightly lower than between M and X - MAV (except for O1) as might be expected since M is derived from the X component. However, the correlations between M and corresponding X and Y octave bands are close enough to corroborate the similarity in the average amplitudes of X and Y already noted.

The correlations between M and Y - MAV by octave band and local hour (see Figure 4) evince considerable variability having an average range from r = 0.465 to 0.800 for all octave bands. Again the complexity of the relationship between M and X - MAV for individual octave bands is obvious. There are several maxima and minima in hourly correlation which persist in three or more octave bands, but it is difficult to attribute physical significance to hourly fluctuations

in correlation of such magnitude. The relative minimum correlation at 1700 LT in all octave bands, Figure 4, is the lowest correlation for each band except O6. There is a possibility that it is due to a peak in the local lightning contribution to M for this five month interval which is dominated by summer months.

The correlation between M and Y - MAV by octave band and local hour is very similar to that for X - MAV. The 1700 LT relative minimum is present in Y also and is the lowest correlation for all octave bands except O5 and O6.

The hourly correlation between M and octave band MAV's provide no clear indication of time dependent period content. As will be seen in the next section, combining the six X - MAV octave bands with proper weighting factors prior to correlation with M improves the correlation for the total data set as expected and smooths the hourly correlation so that local time variations in correlation emerge.

C. Correlation Between M and X - MAVINDX

One reason M and X - MAV did not correlate well is their disparate nature; M, by definition, is a fixed six step index while X - MAV is continuous. Therefore, to partially rectify this inherent dissimilarity, the X - MAV amplitudes were quantized to create a distinct index, X - MAVINDX, having integral values consistent with M. The quantization is based upon the relative occurrence frequency of M values (see Figure 3) for the X - MAV data interval; that is, the relative occurrence frequency of the X - MAV amplitudes for each octave band were normalized to correspond to the six M categories.

10

For example, if 20% of the hourly M's had a value of 1, then the lowest 20% of the X - MAV amplitudes formed the lowest X - MAVINDX category. Similarly, X - MAVINDX categories were established for the remaining M categories. To create a composite X - MAVINDX of the octave bands, it was necessary to weight the X - MAVINOX values appropriately because of the fundamental spectral slope of approximately 6 db/octave which is absent from M.

The coefficients for the correlation between M and X - MAVINDX for the total data set are given by individual octave bands and by successive combinations of weighted octave bands in Table 1. The coefficients for individual octave bands are higher than corresponding ones for the X - MAV correlation. They also exhibit progressively lower correlation with increasing period band with the same implications discussed for r(M, X - MAV). Still higher correlation coefficients for successively combined X - MAVINDX octave bands increase slightly from combinations 01-02 through 01-02-03-04-05-06. Thus, as the octave band data set is combined to better approximate broad band M, the correlation between them improves accordingly.

The correlation coefficients for r(M, X - MAVINDX) by octave band and local hour has a range almost exactly the same as the average range for all octaves for r(M, X - MAV), but the hourly variation is much smoother for corresponding octave bands as can be seen in the lower portion of Figure 5 which gives the envelope of the individual X - MAVINDX octave band coefficients.

11

The upper curve in Figure 5 is the correlation by local hour between M and the composite X - MAVINDX (6 octave bands combined with appropriate weighting) plotted to the same scale as the envelope of individual band coefficients. The composite X - MAVINDX has the highest correlation with M for each local hour and exhibits a rather smooth diurnal variation which is interrupted only by relative minima around local hours 04 and 11-12. The daily maximum correlation is reached at local hour 10 and regained for local hour 13 after the noon time dip. The daily minimum correlation occurs at local hour 19 but is relatively low for local hours 17, 18, 20, 21 and 22.

Despite the broader period band content of X - MAVINDX, some residual difference   period band content is indicated by the diurnal variation in correlation between it and M. The broad daily maximum in correlation, peaking at local hour 10 or 13, suggests that the least divergence in frequency content is attained for these hours. The daily minimum correlation occurs at an auspicious time for short period input to M from local lightning as was more weakly suggested in the correlation between M and horizontal component MAV's. The short period contribution to M from pearl type pulsations could explain the relative minimum at local hour 04 since that time sector favors this fairly rare phenomenon. The local noon time dip in correlation is more difficult to explain because the period band source producing it is not apparent. Extending the period band content of the composite X - MAVINDX, especially to shorter periods, might provide additional insight; but examination of individual hourly spectra is essential to understanding this dip in the final analysis.

D. Correlation Between Octave Band MAV's

The correlation between octave band MAV's was done to check for the existence of singular relationships and to gain insight into both their overall and local time behavior. Correlation coefficients were computed for X and Y for the total data set with and without ap > 48 excluded (see Table 2). The X and Y coefficients, 15 each, for all ap are uniformly high and present no singularities. The comparable set of coefficients for ap > 48 excluded are all lower than the former. There is also a pattern of correlation in that the highest correlations occur between contiguous octave bands while those between increasingly remote bands decrease sharply. Once the domination of ap > 48 values is removed, this pattern is neither surprising nor singular.

Correlation between octave band MAV's by local hour, again with and without ap > 48 excluded, was also completed for X and Y to investigate possible local time dependence. There is a tendency for all octave band pairs to correlate well during local night-time with all ap included. There is also a tendency for a broad minimum in correlation to occur, particularly for correlation pairs involving 01, 02 and 03, near local noon; i.e., between local hours 11 and 15 or 16, with all ap included. These tendencies, the significance of which are clouded by the probable domination by ap > 48 values, disappear in a highly irregular and confusing distribution of hourly coefficients for all octave band pairs with ap > 48 excluded. Thus, a lack of coherent local time dependence is indicated.

13

As in the last section, interpretation of local time behavior of correlation coefficients would be greatly enhanced by examination of hourly spectra. Such spectral analysis was, unfortunately, impossible due to time limitations.

E. Correlation Between ap and Horizontal Component MAV's

The relationship which exists between quasi-sinusoidal geomagnetic variation activity levels and geomagnetic disturbance is important because it may provide a basis for understanding varying states of magnetospheric excitation. To obtain a preliminary impression of this relationship, scatter diagrams of $\log_{10}$ MAV versus $\log_{10}$ ap were prepared for each UT three-hour interval and octave band. The logarithms of the parameters were used to minimize the clustering of points at low MAV and ap values. Since the MAV's are computed over hourly intervals, three-hour means of MAV were used for correlation with ap. Results obtained for X and Y components are quite similar; therefore, only the Y component will be discussed for the sake of brevity.

To a first approximation, the scatter diagrams for any octave band can be separated into two groups according to whether (A) the points for the UT three-hour interval cluster well about a single straight line or (B) about two straight line segments with the high ap segment having the steeper slope. The separation of scatter plots into the two groups by local time sector is as follows: (A) 0400 - 1600 LT and (B) 1600 - 0400 LT. Thus, the (A) group is a local day-time phenomenon while the (B) group occurs during local night-time.

14

It is interesting that the two local time sectors are asymmetric with respect to the noon-midnight meridian plane. This observation can be added to a growing body of experimental evidence which suggest that the magnetosphere is asymmetric about the earth-sun line; e.g., the asymmetric ionospheric current system for SD derived by Silsbee and Vesting (1942), the dawn-dusk asymmetry in low altitude percipitating electrons (E $\geq$ 40 Kev.) found by Hartz and Brice (1967) and the clockwise and counterclockwise polarization zones for scr associated geomagnetic field fluctuations described by Wilson (1962).

Representative scatter diagrams for groups (A) and (B) are shown in Figure 6. Both diagrams are for 01 since the distinction between the groups is most pronounced for the shortest period band; it is progressively weaker for longer period bands. Close scrutinization of 01 to determine which UT three-hour interval possessed the lowest ap value at which the change in slope occurs was accomplished by computing least squares regression slopes and intercepts for the data after empirically partitioning it into ap $\leq$ 48 and ap > 48 subsets. Based upon the two sets of slopes and intercepts, the ap coordinate of the intersection of the two regression line segments was obtained for each UT three-hour interval. The minimum ap coordinate was calculated to be ap = 49 for UT three-hour interval 1. This result must be regarded with great caution because there were only five data points in the ap > 48 subset.

Despite the paucity of data at high geomagnetic disturbance levels for this data set, the results, with due caution, suggest the following:

(1) for local daylight hours 0400-1600, hydromagnetic waves propagate along geomagnetic field lines which are entirely within the inner magnetosphere and produce geomagnetic micropulsations the amplitudes of which increase at an essentially constant rate with progressively increased disturbance levels and (2) for local night-time hours 1600-0400, a threshold in the geomagnetic activity level exists, especially for shorter period bands, beyond which the rate of change of micropulsation amplitudes with increasing disturbance is greater than for quiet to moderate conditions. One possible explanation for (2) is that during intervals of enhanced magnetospheric excitation the inflated tail field lines extend to lower geomagnetic latitudes providing efficient guiding for short period waves but progressively less effective guiding for longer period waves as they approach the earth due to strong geomagnetic grandient induced mode coupling. Thus, increasing levels of magnetospheric excitation, particularly in the local night-time sector, apparently bring the low latitude limit of closed inner field lines nearer to the Concord field station's geomagnetic latitude making it more accessible to perturbations generated in the magnetospheric neutral sheet and to plasma cusp instabilities.

Finally, two observations will be made concerning UT three-hour intervals for which ap $\leq$ 48, i.e., intervals for which hydromagnetic wave propagation observed at the Concord station is confined to the closed geomagnetic field lines of the inner magnetosphere which do not participate in the bulk convective motions through the magnetotail.

The first observation, illustrated in Figure 7, relates to the diurnal variation in the linear correlation between ap and X - MAV. It can be seen that, for the two shortest period bands, the correlation is maximum for local hours 22-01 and 01-04, respectively, while the minima for both occur near local noon. No consistent pattern exists for the remaining octave bands although 03, 04 and 06 do have peak correlations for local hours 01-04 and 10-13. The physical implications of these diurnal patterns are not at all obvious. Post-midnight maxima (0100-0400 LT) in correlation might be attributed to energetic particle precipitations such as those observed by Hartz and Brice (1967). They found these events to be statistically associated with moderately intense electron fluxes ($E \geq 40$ Kev.); with strong slowly varying riometer absorption and with characteristically hard X-ray events. The pre-noon maxima for the 03, 05 and 06 bands could originate in enhanced hydromagnetic wave generation at the sunward magnetopause during relatively disturbed conditions.

The second observation pertains to the rate of change of X - MAV as a function of ap which is represented by least squares regression line slopes for these parameters. Figure 8 shows the diurnal variation in slopes for all octave bands. The greatest sensitivity (maximum rate of change) of X - MAV with respect to ap is prior to local noon for 01 and 02 and then shifts to afternoon for the remaining octave bands, becoming progressively later in passing from 03 to 06. Secondary maxima exist for 05 and 06 at 0400-0700 LT. The diurnal behavior of 01 and 02 follows closely that of

17

the M index over a much longer time interval reported on by Frey
et al. (1970). The broad day-time maxima in slope displayed by these
shorter period bands is, again, probably due to sustained excitation
of the sunward magnetopause which provides an energy source for
hydromagnetic waves. The physical significance of the variation
patterns of regression line slopes for O5 and O6 will require further
investigation if they are to be understood.

5. Spectral Enhancements

One of the primary aims of this investigation was to establish
whether any portion of the quasi-sinusoidal geomagnetic variation
amplitude spectrum contains significant and consistent departures
from a simple inverse frequency dependence and if so to determine
the local time behavior of such departures.

Spectral enhancements (SE's) are difficult to determine in detail
without inspecting individual spectra for each of the more than 3000
hours of data analyzed. A less detailed and consequently more
limiting approach was adopted to make the search for SE's feasible.
Initially, a computer program was created to scan the horizontal
component data sets and record hourly SE occurrences. An SE in a
particular octave band, Oi, is defined by the simple condition
APSD Oi > APSD $Oi+1$. Thus, by definition, only a pronounced energy
increase over an octave band width will be considered an SE and, of
course, it is impossible to resolve SE's in O5, the longest period
octave band.

The hourly spectrum shown in Figure 9 is a particularly good example of an SE in 03 and, as discussed below, is a prominent feature of the local time hourly spectra for both the X and Y component geomagnetic variations. The salient features of the SE analysis are illustrated by relative occurrence frequency tables and, since the results obtained for X and Y are quite similar, the discussion is confined to the X component tables.

The SE's are essentially a local day-time phenomenon. They are well distributed in time over the total data interval as evidenced by the fact that 119 of the 141 days analyzed had at least one SE. On the other hand, very few hours had multiple SE's, i.e., SE's in different octaves for that hour. Of all hours for which SE's were found, only 4% had two SE's in the same hour and over half of them involved contiguous octaves, specifically the 02, 03 and 03, 04 pairs. Thus, SE's for any hour are preferentially confined to one octave.

The SE's exhibit a relatively strong persistence tendency, that is, a tendency for consecutive hours to contain SE's in the same octaves. For hours having at least one SE, 34% are followed by hours having an SE in the same octave.

Table 3 summarizes several properties of the SE occurrence frequency by octave band. The first line of this table shows the relative occurrence of SE's for all hours in the total data set. SE's in 03 are most frequent, at least 3 times more frequent than SE's in any other octave band. Line two of the table demonstrates

19

Hourly occurrence percentages of concurrent SE's in corresponding octaves of X and Y are also presented in Table 5. The diurnal variation of these occurrences is similar to that described above. Here the occurrence pattern suggests minimum coupling between X and Y during local hours 16-21.

Finally, a weak recurrence tendency is educed when daily sums of the numbers of SE's for all hours and any octave are plotted in successive 27-day (solar rotation period) intervals. Figure 10 is a plot of the daily total SE's for four successive 27-day periods commencing on 12 April 1967. A recurrence tendency is weakly suggested by the plausible alignment of corresponding maxima and minima in the successive 27-day patterns. Similar plots of the equivalent daily planetary amplitude, Ap, which is a measure of overall geomagnetic disturbance, are shown in Figure 11 for comparison. It is clear that no recurrence tendency exists during this time period in overall geomagnetic activity. Hence, there is the suggestion that SE's are somehow sensitive indicators of interplanetary conditions not apparent in measures of overall magnetospheric excitation.

6. Events Based Upon ap Sequences

The cause for preferential occurrence of SE's in O3 must be uniquely related to overall geomagnetic activity. Hence, this cause will be pursued. The SE selection criterion of Section 5 resulted in relatively few cases; therefore, a less restrictive criterion is selected here to

21

provide more cases. Instead of using the difference between O4 and O3, the ratio O4/O3 (of the same spectral values) is used as a relative measure of SE's in O3. The SE's of Section 5 would produce ratios less than 1 with this less restrictive selection criterion. Additionally, only time intervals having low geomagnetic disturbance levels (ap ≤ 7) for at least six successive UT 3-hour intervals followed by abrupt increases sustained for a minimum of four succeeding UT 3-hour intervals are selected. For all of the intervals satisfying the conditions above, ap increased by at least a factor of 2 in going from the last 3-hour interval of the undisturbed portion to the first 3-hour interval of the "disturbed" portion. The resulting 15 step-function-like events in geomagnetic activity are well distributed over the total sample time interval and are individually separated by a minimum of four days. Table 6 contains the dates and UT hours for which the abrupt increases in geomagnetic disturbance occurred in each event.

The O4/O3 ratios were initially organized into a superposed epoch table such that the zero 3-hour interval contained the first high ap value in the sequence of 3-hour intervals. The six undisturbed intervals before the zero interval are numbered from -1 backward to -6 while the three "disturbed" intervals following it are numbered forward from +1 to +3.

Prior to columnwise averaging to obtain a superposed epoch curve, the O4/O3 ratio for each hour in each event was adjusted to minimize biasing due to the mean diurnal variation in SE occurrences previously discussed. The adjustment was accomplished by computing the mean

diurnal variation of the O4/O3 ratio utilizing data from the total sample and then applying the reciprocal of the hourly mean diurnal variation as a weighting factor to corresponding hours in the super-posed epoch table. This adjustment, although only approximate, is essential because of the non-uniform distribution of geomagnetic disturbance over the Greenwich day which contributes potentially non-canceling values from events with identical zero intervals to the columnwise averages. This latter point is clarified by an inspection of Table 6 which shows that five of the fifteen events have their zero intervals centered on UT hour 2.

After adjusting each entry in the superposed epoch table by its appropriate weighting factor, the ratios were averaged over 3-hour UT invervals for comparison with the corresponding ap mean values obtained by averaging over the fifteen events. The final results for both ap and the adjusted mean ratios are shown in Figure 12. It is to be emphasized again that low values of the adjusted O4/O3 ratios are only relative measures of SE's in C3 above the otherwise "red" background spectrum.

The most important result of this analysis is that the greatest tendency for SE's to occur in O3 is approximately 9 hours before the abrupt increase in world-wide geomagnetic disturbance and that the tendency is relatively low during the period of high activity. This result suggests the existence of a readily measured precursor to world-wide enhancement in geomagnetic activity.

This section will be concluded by relating the observation above
to conditions which are assumed to exist in the interplanetary medium.
The interplanetary medium can be grossly divided in the ecliptic into
sectors of slow and fast solar wind flow with the thin boundary between
them being a region of shear turbulance. While the magnetosphere is
immersed in the sector of low solar wind velocity, the geomagnetic
disturbance and micropulsation activity levels should be relatively
low (Snyder et al., 1963) and (Frey et al., 1970). When this sector
sweeps past the magnetosphere, the turbulent boundary region should
then be encountered which should generate hydromagnetic waves (micro-
pulsations) but should not appreciably affect world-wide disturbance
levels. Finally, the magnetospheric encounter with the sector of
high solar wind velocity following the turbulent region should provide
sufficient energy to abruptly raise the overall geomagnetic disturbance
level (see again Snyder et al., 1963). The subsequent chaotic state
of magnetospheric excitation is apparently not conducive to the genera-
tion of reasonably steady quasi-sinusoidal micropulsations.

Some support for the oversimplified view presented above is found
in the results of Sari and Ness (1968), who found that the power spectra
of the interplanetary magnetic field (based on Pioneer 6 data) con-
sistently exhibit a frequency dependence with power proportional to f^{-2}
(similar to the background spectrum reported here) and also exhibit
statistically significant spectral peaks during quiet geomagnetic
conditions some of which have periods of 80 and 120 seconds. They
attribute the dominant 6db/octave spectral trend to interplanetary

field directional discontinuities and the position of the spectral peaks to the magnitude and spacing of these discontinuities. It is certainly conceivable that the discontinuities would be more numerous in the turbulent boundary region separating the slow and fast streams and that the occurrences of SE's in O3 are a manifestation of the presence of this region as it sweeps past the magnetosphere. The apparent nine hour time lag might then be considered as an indirect measure of the boundary region thickness in the ecliptic plane. Furthermore, the preference of SE's for O3 (T=64-128 sec.) might be an expression of a characteristic spacing between directional interplanetary magnetic field discontinuities in the solar wind. Finally, it is also plausible that these discontinuities, after interacting with the magnetopause, are most efficient in generating hydromagnetic waves near the earth-sun line, i.e., the forward stagnation point and the "open" magneto-tail. Recall (Table 4) that the SE occurrence frequency in O3 has primary and secondary maxima near local noon and midnight, respectively.

The speculative depiction of the interaction between interplanetary and magnetospheric phenomena advanced above is, of course, based on preliminary impressions which assume that the driving mechanism resides in spatial discontinuities in the interplanetary magnetic field. The apparent delay between energy enhancements in O3 and overall geomagnetic disturbance might also arise (either totally or partially) from internal magnetospheric processes such as quasi-periodic particle precipitation events or resonant hydromagnetic wave perturbations associated with the plasmapause. In any case, the creation of a larger data set possessing

more step-function-like ap events would produce a more uniform distribution of ʄ magnetic disturbance over the Greenwich day, would obviate the necessity for adjustment and would enhance the reliability of the resultant impressions. Likewise, parallel analysis of SE's in other octave bands would provide a test for the preliminary impressions and might strengthen them.

7. Ratio RMS/MAV (Stationarity)

As indicated at the outset of this report, the octave bandwidth APSD and MAV estimates were computed over hourly intervals. The use of the ratio RMS/MAV to gain insight into the nature of quasi-sinusoidal geomagnetic variations over intervals less than one hour will now be described. The RMS value is obtained by computing the square root of the product of the APSD and the bandwidth.

It is of particular interest to establish whether the data for a given hour represents a stationary or non-stationary stochastic process. Inspection of oscillographic records of the variations clearly indicates non-stationarity in the time varying mean square value sense because long temporal trends were removed by analog filtering prior to digitization of the data.

Ratios of RMS/MAV were calculated for three idealized signals using the probability density distributions for them: (a) a sinusoidal signal with random phase, RMS/MAV = 1.11; (b) a signal having uniform probability density distribution, RMS/MAV = 1.15; and (c) a signal characterized by a Gaussian distribution, RMS/MAV = 1.25.

Time intervals containing intermittent and isolated "spikes" can be approximated by a signal having a discrete probability density distribution. The value of the ratio for this class of signals is variable depending upon the relative amplitude and number of "spikes" in the interval. Ratios in the range 1.5 and 2.0 are typical for hours displaying short duration burst type pulsations.

The occurrence frequency by octave band of hours having RMS/MAV ratios from 1.0 to 3.0 was computed for small incremental steps. The percentage occurrence of hours for which RMS/MAV > 1.5 are as follows:

01	9.1%	04	3.6%
02	11.7%	05	1.7%
03	11.9%	06	0.9%

It is obvious that the geomagnetic variations become more stationary with increasing period bands. The maximum non-stationarity is for 02 and 03, T = 32-128 sec. This period range is nearly coincident with the IAGA irregular pulsation class Pi2 which is 40-150 sec.

Hourly mean ratios over the Greenwich day were also generated. These ratios are presented by octave band in Figure 13. The diurnal variations displayed by the mean ratios for 01, 02 and 03 are similar in that all suggest the existence of impulsive burst type pulsations during local hours 22-01 and the presence of more steady continuous pulsations prior to local noon. The secondary maximum around local hour 14 is probably of dubious physical significance. The hourly fluctuations for 04, 05 and 06 mean ratios exhibit no clear diurnal variation. Thus, impulsive burst type micropulsations are chiefly

confined to shorter period bands (T < 128 sec.) and tend to occur in the hours prior to local midnight. Also, the results of other analysis not described here indicate a lack of dependence of the RMS/MAV ratio on geomagnetic disturbance.

The principal value of the RMS/MAV ratio is as a selection and reliability device. Traditional power spectral density analysis, which involves preliminary computation of the auto-correlation function, is strictly valid only for stationary data. Therefore, delineation of auspicious or inauspicious data for power spectral density analysis depends upon the determination of its degree of stationarity. The degree of confidence to be placed in power spectral density estimates also depends on the degree of stationarity of the data. The RMS/MAV ratio facilitates such a determination. Furthermore, this ratio is quite sensitive to the presence of artificial (noise) transients which must be eliminated to prevent contamination of the natural variations.

8. Computer Programs

Numerous computer programs were created during the contract period in order to reduce, edit and analyze the octave band width data set. A brief identification and functional description for each program is as follows:

CNVMK

Input: IBM 7094 DCS tape file MKTAPE

Output: CDC 6600 compatible tape file EM-MKTAPE

Function: To convert the IBM 7094 binary tape file containing geomagnetic micropulsation and magnetic disturbance indices into a binary tape file compatible with the CDC 6600 computing system.

CNVLOW

Input: IBM 7094 DCS tape files of the LOW Series

Output: CDC 6600 compatible tapes of the EMLOW Series

Function: To convert IBM 7094 binary tape files containing low pass filtered data into binary tape files compatible with the CDC 6600 computing system.

FILTER

Input: Binary tape files of the EMLOW Series

Output: Punched-card file

Function: To obtain hourly estimates of the average power spectral density and mean absolute value of geomagnetic micropulsations over contiguous octave frequency bands.

CDTPE

Input: BCD card image tape file

Output: Binary tape file containing power spectral density estimates and a binary tape file of mean absolute values.

Function: To merge card images for a given component and sensitivity (eg. YL) and generate separate tapes for the power spectral density and mean absolute value; to provide error checking for mis-punched cards and for out-of-sequence cards.

MERGE

    Input: Binary tape file of mean absolute values

    Output: Updated binary tape file of mean absolute values

    Function: To include in the appropriate tape files mean absolute
values which were punched by the CDC version of program
FILTER.

OVRLD

    Input: Binary tape files of high and low sensitivity mean
absolute values and high and low sensitivity power
spectral density estimates

    Output: Printout

    Function: To delineate hours during which the data are contaminated
by overloading; the selection criterion was based upon
the ratio of the mean square value to the square of the
mean absolute value for both the high and low sensitivity
data for each octave.

COMPS 1

    Input: Punched cards containing basic calibration scalings for
each primary data set.

    Output: Printout

    Function: To compute 1967 data conversion factors (gamma/millivolt)

OVLDCRD

    Input: Binary tape file of low sensitivity power spectral density
estimates

    Output: Punched card file; printout

Function: To correct low sensitivity RMS values for background noise during intervals considered overloaded; to punch overload substitution cards acceptable as input to program FIXOVLD.

FIXOVLD

Input: Uncorrected mean absolute value tape file; punched card file

Output: Final mean absolute value tape file; printout

Function: To delete extraneous hours at the end of individual data samples; to multiply both high and low sensitivity data by normalization constants based upon mean conversion factors (gamma/millivolt) for the 1967 data set; to substitute noise-adjusted low sensitivity data for high sensitivity data during hours observed to be overloaded.

PRMKA

Input: Binary tape files EM-MK and EM-AXDY

Output: Printout

Function: To obtain a composite printout by day of daily average Ap, 8 Ap's, 8 Kp's, 8 Kfr's, 24 M's and the 24 mean absolute values for each of the six octave bands.

CORCOMP

Input: X and Y component mean absolute value tape files

Output: CRT plots; printout

Function: To determine extent of linear product moment correlation between the two horizontal component channels.

31

MCORAVE

    Input: Mean absolute value tape file; tape file EM-MK

    Output: CRT plots; printout

    Function: To correlate the one-hour micropulsation index with

           either the X or Y mean absolute value data set.

CORROCT

    Input: Mean absolute value tape file EM-AXDY or EM-AYDY

    Output: CRT plots, printout

    Function: To ascertain the degree of linear product moment

           correlation between all possible octave band combinations

           for a given component.

MDIST

    Input: Tape file EM-MK

    Output: Printout

    Function: To obtain a frequency distribution of $M(1-6)$ for the

           total data sample and also by hour; to correct M

           values originally mis-scaled.

OCTINDX

    Input: Tape file EM-AXDY and tape file EM-MK; punched cards .

    Output: Printout

    Function: To read mean absolute value frequency class limits from

           punched cards in order to convert each continuous mean

           absolute value into a corresponding discrete value

           ranging from 1-6; to correlate the discrete mean absolute

           value index with the M index separately by octave band

           and in successive weighted combinations of octave bands.

POWRAT

Input: Tape file EM-AXDY

Output: Printout

Function: To compute contiguous octave bandwidth ratios;
to compute for each hour the geometric mean of
the five bandwidth ratios for use as an estimate
of the averaged spectral slope for that hour.

AVEKCOR

Input: Mean absolute value tape file; tape file EM-MK

Output: CRT plots; printout

Function: To generate correlation coefficients and least
squares regression line slopes and intercepts
for corresponding sets of geomagnetic disturbance
indices and mean absolute value estimates for
the X and Y components; to tabulate occurrence
frequency distributions of the mean absolute values
averaged over UT three-hour intervals as a function
of Kp level and UT hour.

BUMP

Input: Tape file EM-AXDY or EM-AYDY

Output: Printout

Function: To indicate the presence of strong spectral enhance-
ments (bumps) in the data based on the relative
magnitudes of the mean absolute values in contiguous
octave bands.

33

RMSMAVK

    Input: Tape files EM-RX, EM-AX and EM-MK

    Output: Printout

    Function: To calculate ratios of the RMS value to the
corresponding mean absolute value and present
mean ratios tabulated according to Kp level and
UT hour for each octave band.

RATIO

    Input: Tape files EM-RX and EM-AX

    Output: CRT plots; printout

    Function: To generate occurrence frequency statistics by
UT hour and mean diurnal variation curves for
the ratio X-RMS/X-MAV for all octave bands.

SPECKPH

    Input: Tape files EM-AXDY and EM-MK

    Output: Printout

    Function: To normalize each hourly spectrum to the value of
octave 06 for that hour and to print a tabulation
of mean normalized spectra by UT hour and by Kp
level.

TABLE 1.

	01	02	03	04	05	06
r(X, Y)	.958	.903	.947	.951	.915	.842
r(X, Y) ap 48 excluded	.882	.806	.763	.733	.656	.477
r (M, X-MAV)	.696	.691	.577	.473	.506	.419
r(M, X-MAV) ap 48 excluded	.703	.606	.519	.450	.475	.409
r(M, X-MAVINDX)	.757	.749	.699	.658	.636	.580
r(M, X-MAVINDX) composite		.810	.822	.834	.838	.840
r(ap, X-MAV)	.779	.812	.836	.837	.816	.754
r(ap, X-MAV) ap 48 excluded	.301	.302	.385	.544	.473	.523
r(ap, Y-MAV)	.693	.764	.818	.806	.821	.835
r(ap, Y-MAV) ap 48 excluded	.299	.280	.406	.528	.517	.590

TABLE 2.

All ap

X	02	03	04	05	06
01	.925	.899	.844	.850	.844
02		.944	.901	.893	.870
03			.922	.901	.878
04				.972	.882
05					.908

Y	02	03	04	05	06
01	.948	.903	.906	.857	.833
02		.958	.932	.897	.869
03			.958	.926	.902
04				.950	.916
05					.908

ap 48 excluded

X	02	03	04	05	06
01	.674	.573	.373	.314	.294
02		.748	.456	.423	.376
03			.725	.599	.501
04				.742	.656
05					.833

Y	02	03	04	05	06
01	.700	.561	.423	.427	.311
02		.708	.427	.421	.347
03			.669	.583	.444
04				.803	.609
05					.708

TABLE 3.

	01		02		03		04		05	
	X	Y	X	Y	X	Y	X	Y	X	Y
% Occurrence of SE's for all hrs.	1.3	0.7	2.2	3.0	7.1	6.7	2.7	2.6	1.3	2.2
% Occurrence of SE's in groups of consecutive hrs.	68	39	55	62	58	56	24	34	15	29
Ave. Duration of SE's in hrs.	1.7	1.4	1.6	1.7	1.7	1.6	1.2	1.3	1.1	1.2
% Occurrence of hrs. with SE's in one component which are also in other component	39	70	55	39	42	44	28	29	17	10

TABLE 4.

Percentage Distribution of SE's

UT	LT	01 X	01 Y	02 X	02 Y	03 X	03 Y	04 X	04 Y	05 X	05 Y
1	20	9.1	0	0	9.1	36.4	36.4	54.5	36.4	0	18.2
2	21	0	0	0	0	42.9	45.5	57.1	54.5	0	0
3	22	0	0	6.7	0	66.7	58.3	26.7	41.7	0	0
4	23	0	0	10.5	16.7	36.8	25.0	42.1	50.0	10.5	8.3
5	24	0	C	0	7.7	61.9	69.2	33.3	23.1	4.8	0
6	1	0	0	0	0	61.5	61.1	38.5	33.3	0	5.6
7	2	0	0	8.3	15.0	50.0	45.0	41.7	30.0	0	10.0
8	3	14.3	0	28.6	4.8	35.7	76.2	14.3	14.3	7.1	4.3
9	4	15.8	9.1	42.1	22.7	26.3	40.9	5.3	22.7	10.5	4.5
10	5	25.0	0	25.0	31.3	43.8	37.5	0	25.0	6.3	6.3
11	6	19.0	10.0	23.8	13.3	23.8	33.3	14.3	20.0	19.0	23.3
12	7	15.4	4.0	23.1	24.0	23.1	48.0	38.5	8.0	0	16.0
13	8	0	8.7	23.5	26.1	70.6	43.5	0	8.7	5.9	13.0
14	9	4.2	4.2	12.5	29.2	62.5	50.0	20.8	4.2	0	12.5
15	10	3.4	3.6	13.8	32.1	69.0	50.0	6.9	0	6.9	14.3
16	11	7.7	13.5	19.2	24.3	57.7	37.8	7.7	2.7	7.7	21.6
17	12	8.6	5.7	11.4	31.4	62.9	42.9	.7	8.6	14.3	11.4
18	13	5.0	3.4	17.5	27.6	57.5	37.9	10.0	17.2	10.0	13.8
19	14	10.0	3.8	20.0	38.5	56.7	42.3	6.7	3.8	6.7	11.5
20	15	18.2	6.9	27.3	17.2	45.5	37.9	4.5	17.2	4.5	20.7
21	16	21.7	0	4.3	5.3	43.5	47.4	13.0	15.8	17.7	31.6
22	17	21.4	5.9	C	11.8	21.4	35.3	28.6	11.8	28.6	35.3
23	18	10.0	14.3	10.0	14.3	10.0	0	30.0	28.6	40.0	42.9
24	19	0	0	0	0	16.7	0	66.6	100	16.7	0

38

TABLE 5.

UT	LT	Percentage of hours of total sample with at least one SE		Percentage of hours with at least one SE in corresponding X and Y octave bands
		X	Y	
1	20	7	8	1.4
2	21	5	8	1.4
3	22	11	9	4.3
4	23	14	9	4.3
5	24	15	9	6.5
6	1	9	13	7.2
7	2	9	14	6.5
8	3	10	15	2.2
9	4	13	16	4.3
10	5	12	12	4.4
11	6	16	21	6.7
12	7	9	19	3.8
13	8	13	18	6.2
14	9	19	21	7.7
15	10	23	23	13.8
16	11	19	30	11.0
17	12	25	24	11.2
18	13	28	21	10.0
19	14	23	20	8.7
20	15	17	21	7.9
21	16	17	14	6.2
22	17	10	13	1.5
23	18	7	5	0.7
24	19	9	1	0.7

TABLE 6.

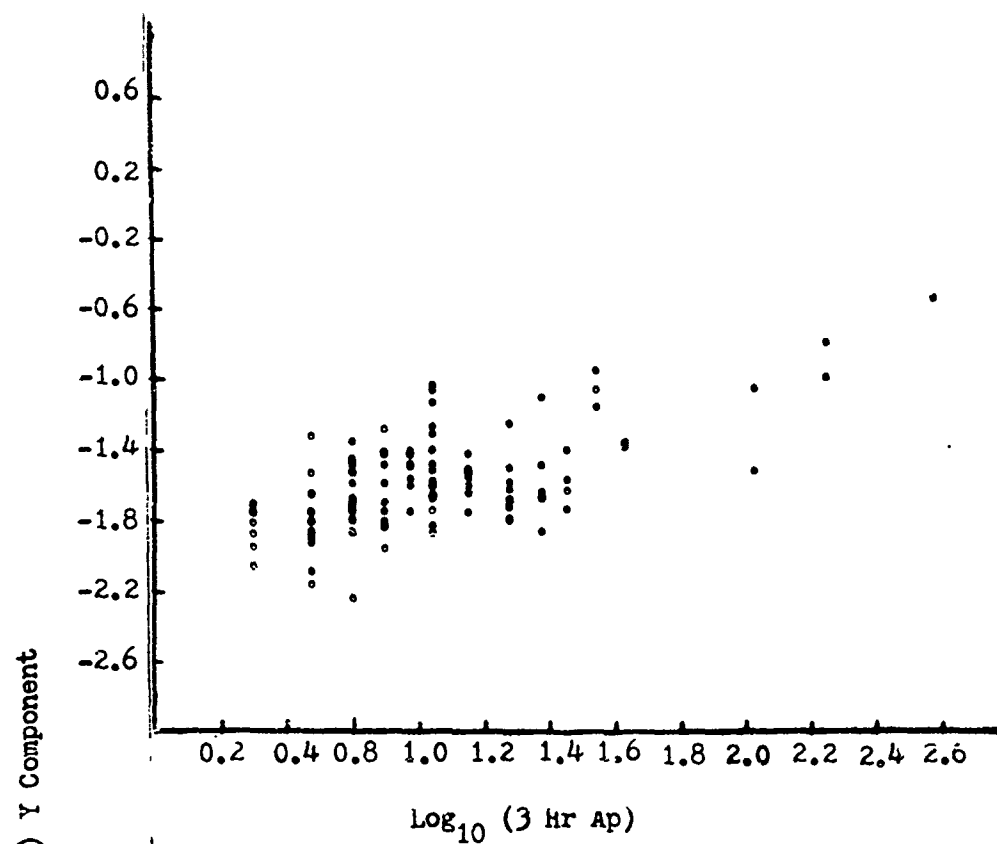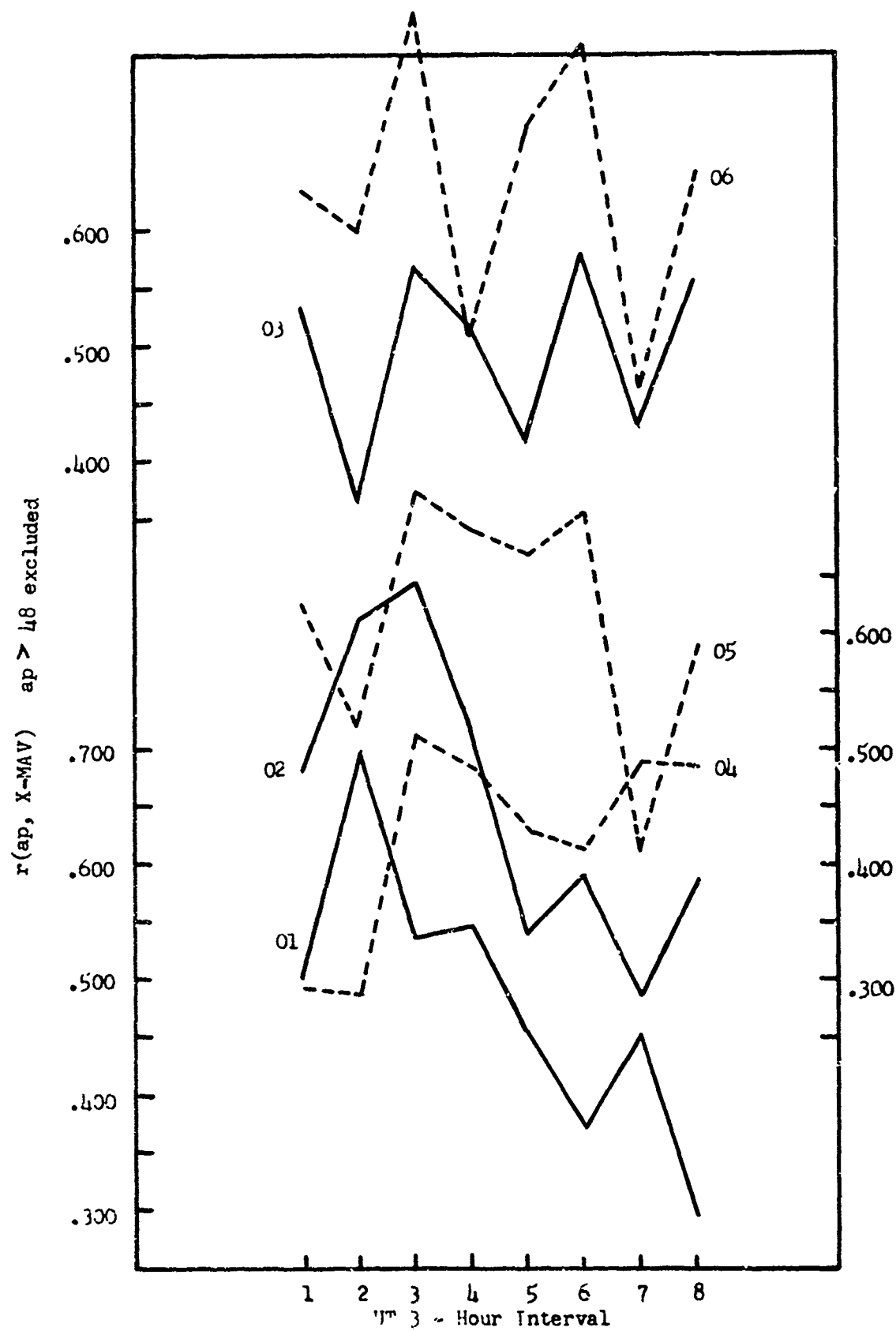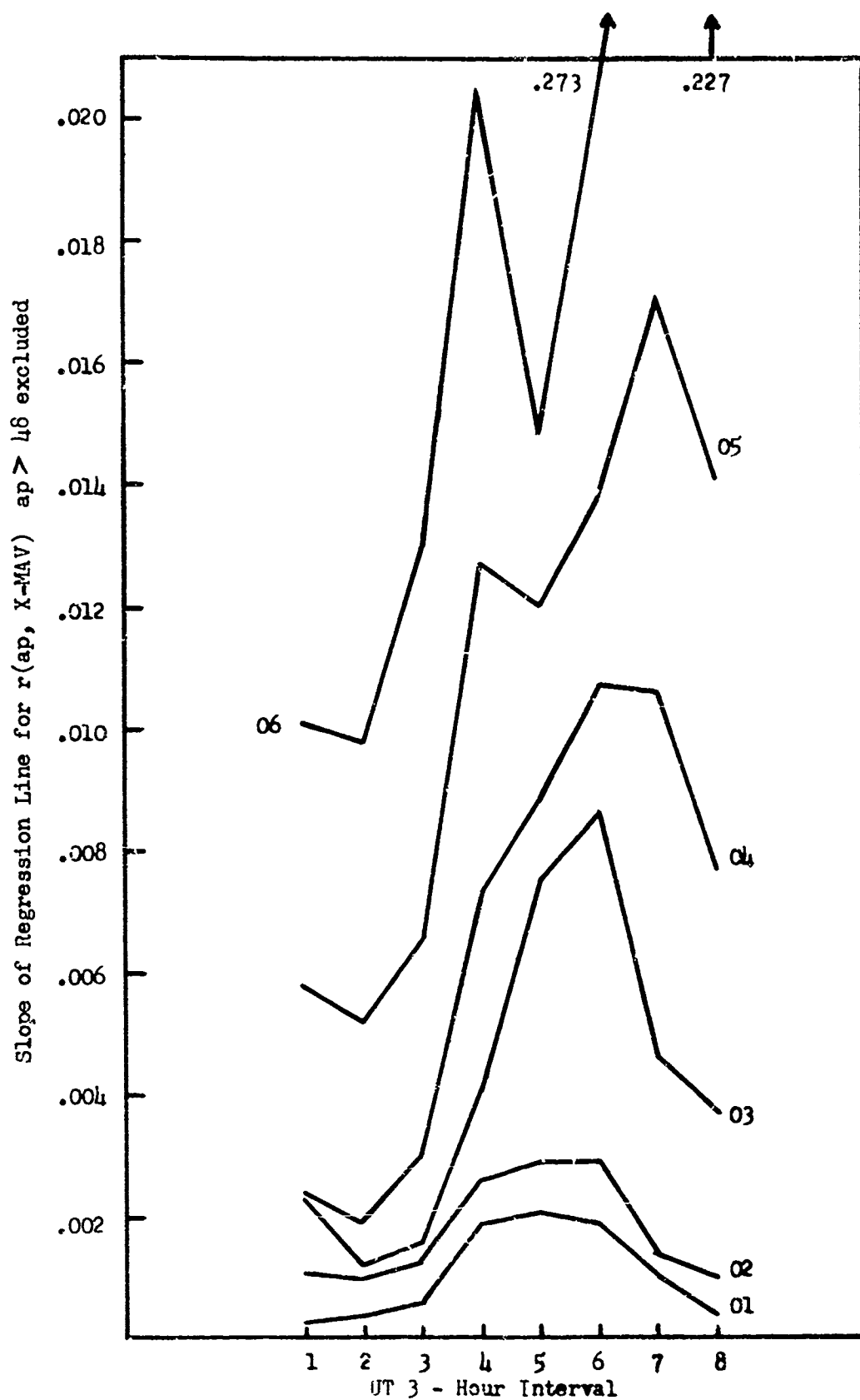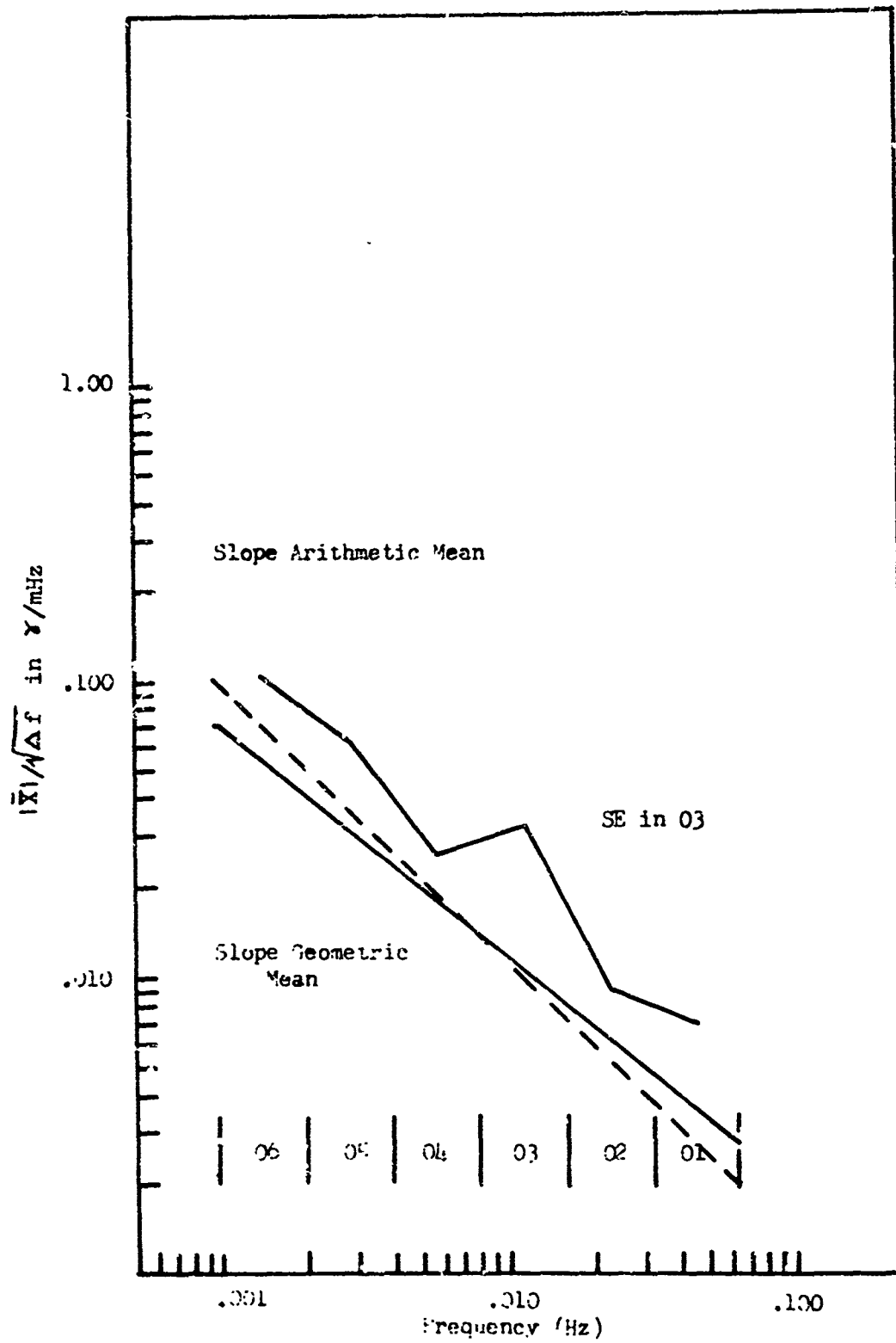| Event No.	Month/Day	UT Hour
1	4/18	23
2	4/22	2
3	5/01	20
4	5/07	2
5	5/11	2
6	5/23	20
7	6/08	11
8	6/14	2
9	6/25	17
10	7/04	23
11	7/11	2
12	7/23	17
13	7/28	14
14	8/07	20
15	8/16	23
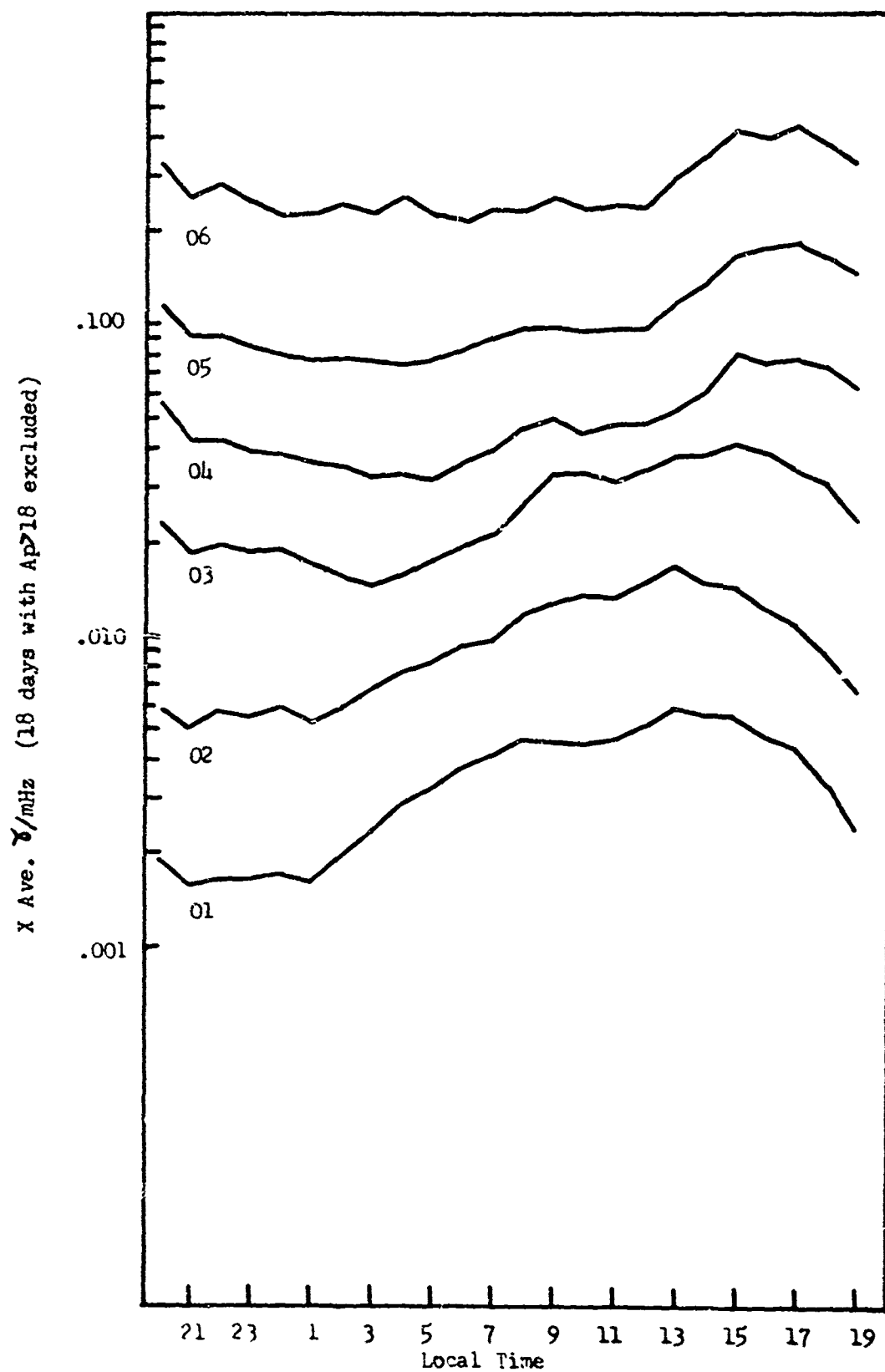
Figure 1.

41
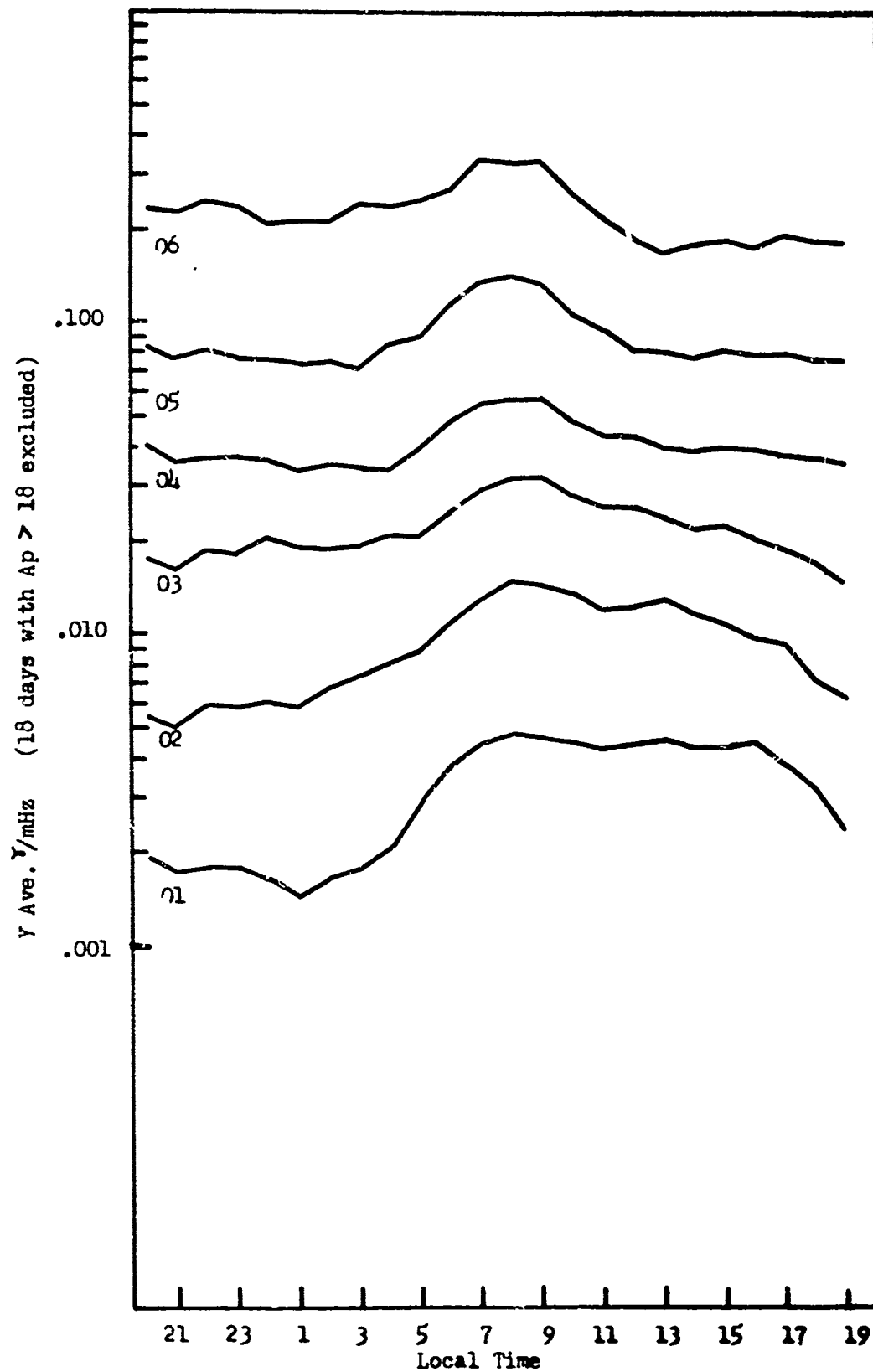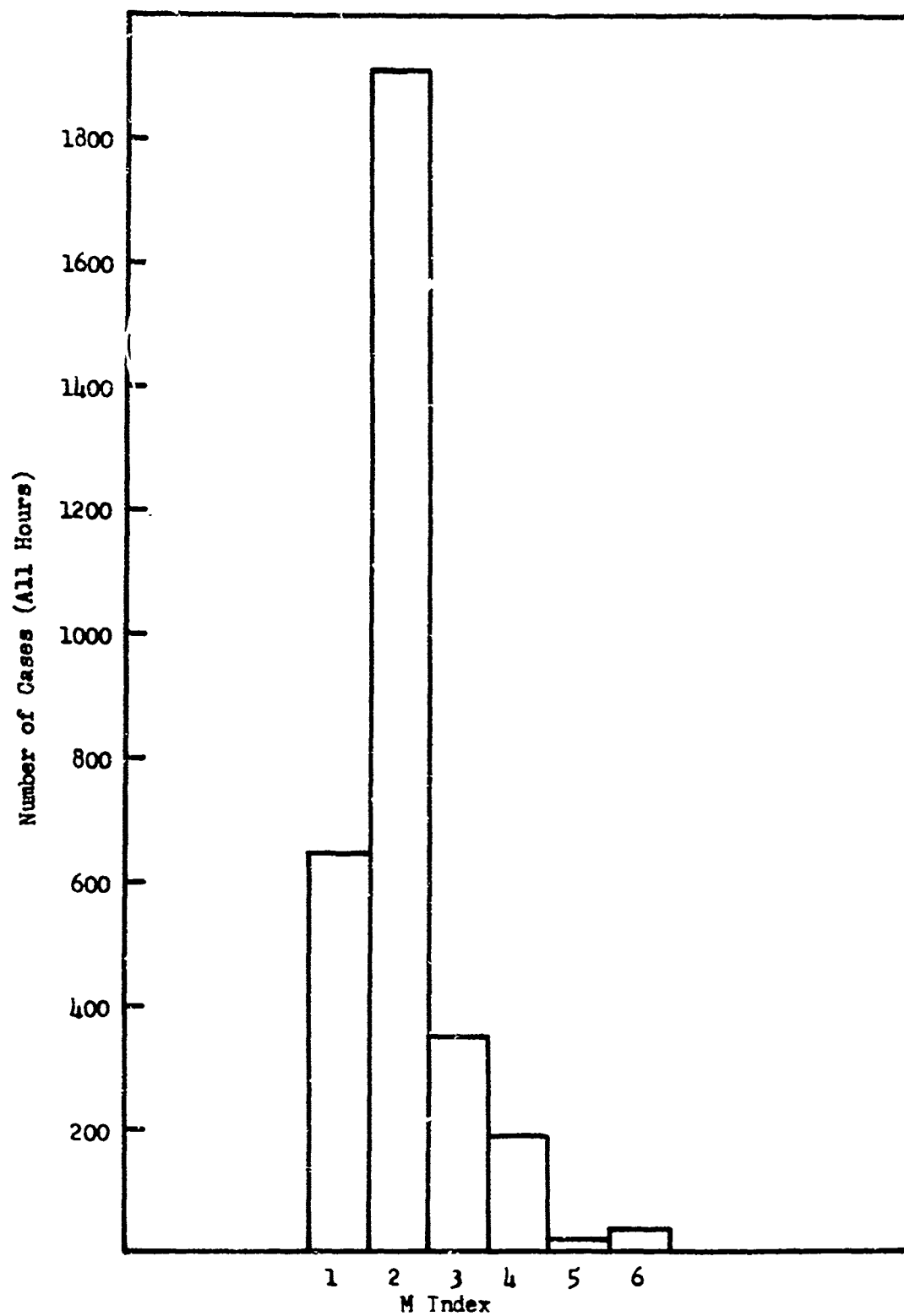
Figure 2.

Figure 3.

Figure 4.

Figure 5.

45

Figure 6

52
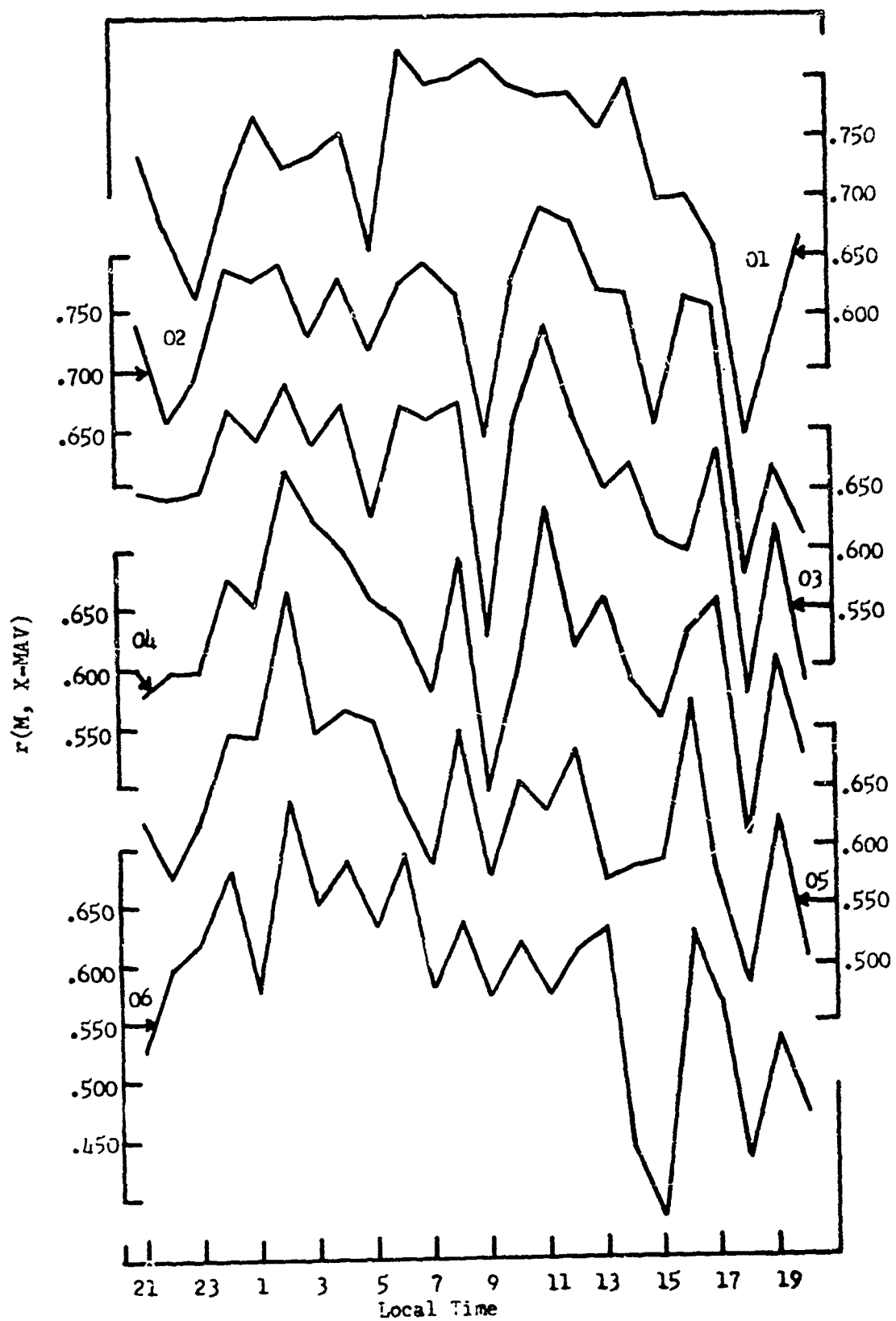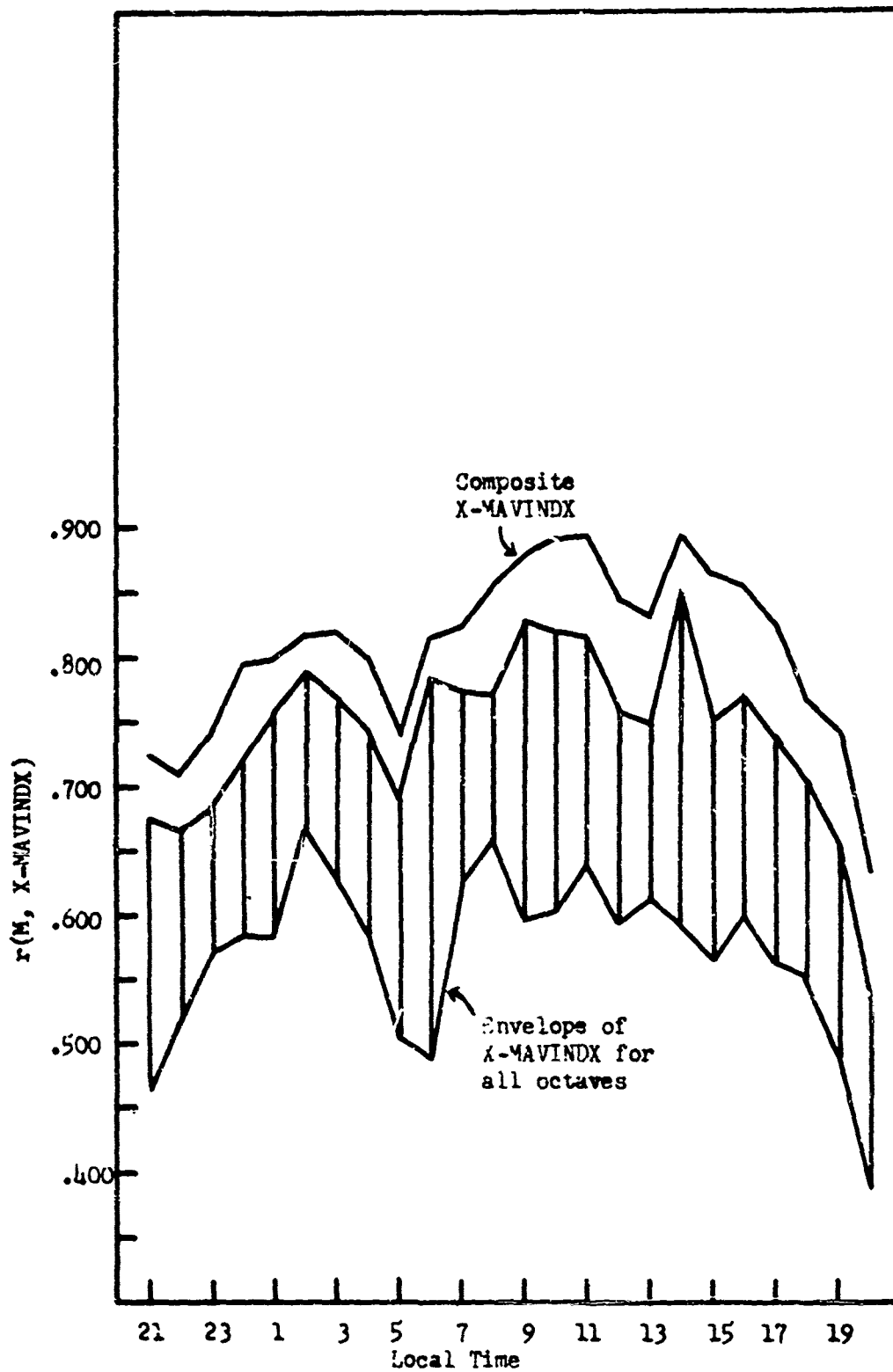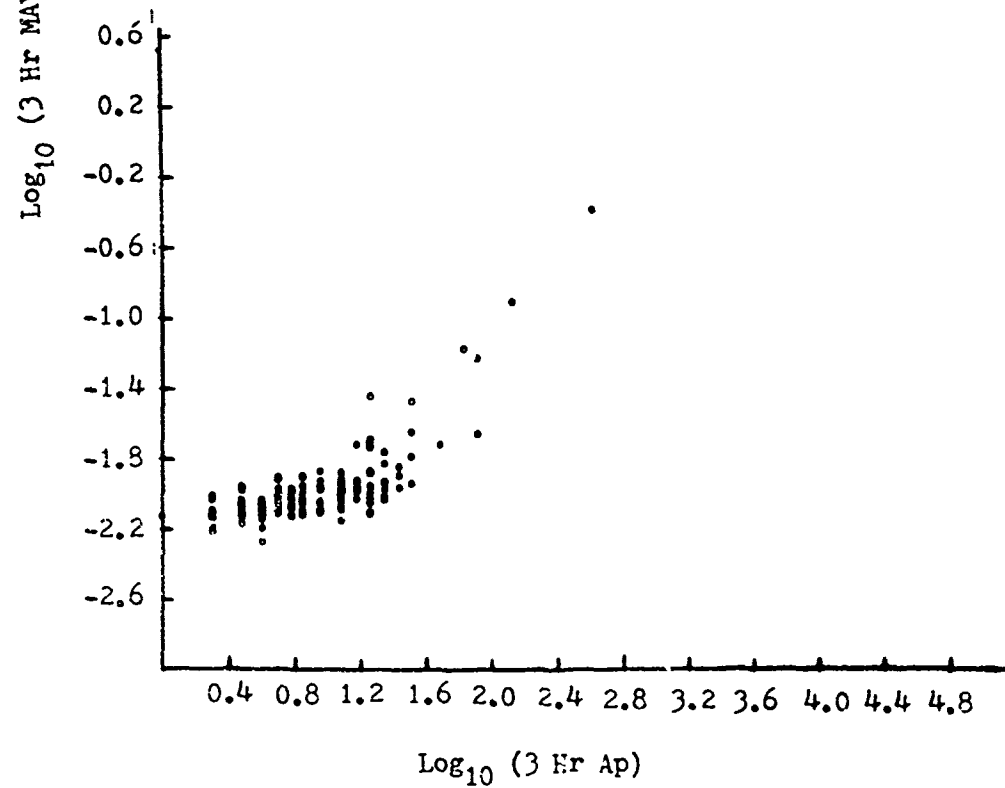
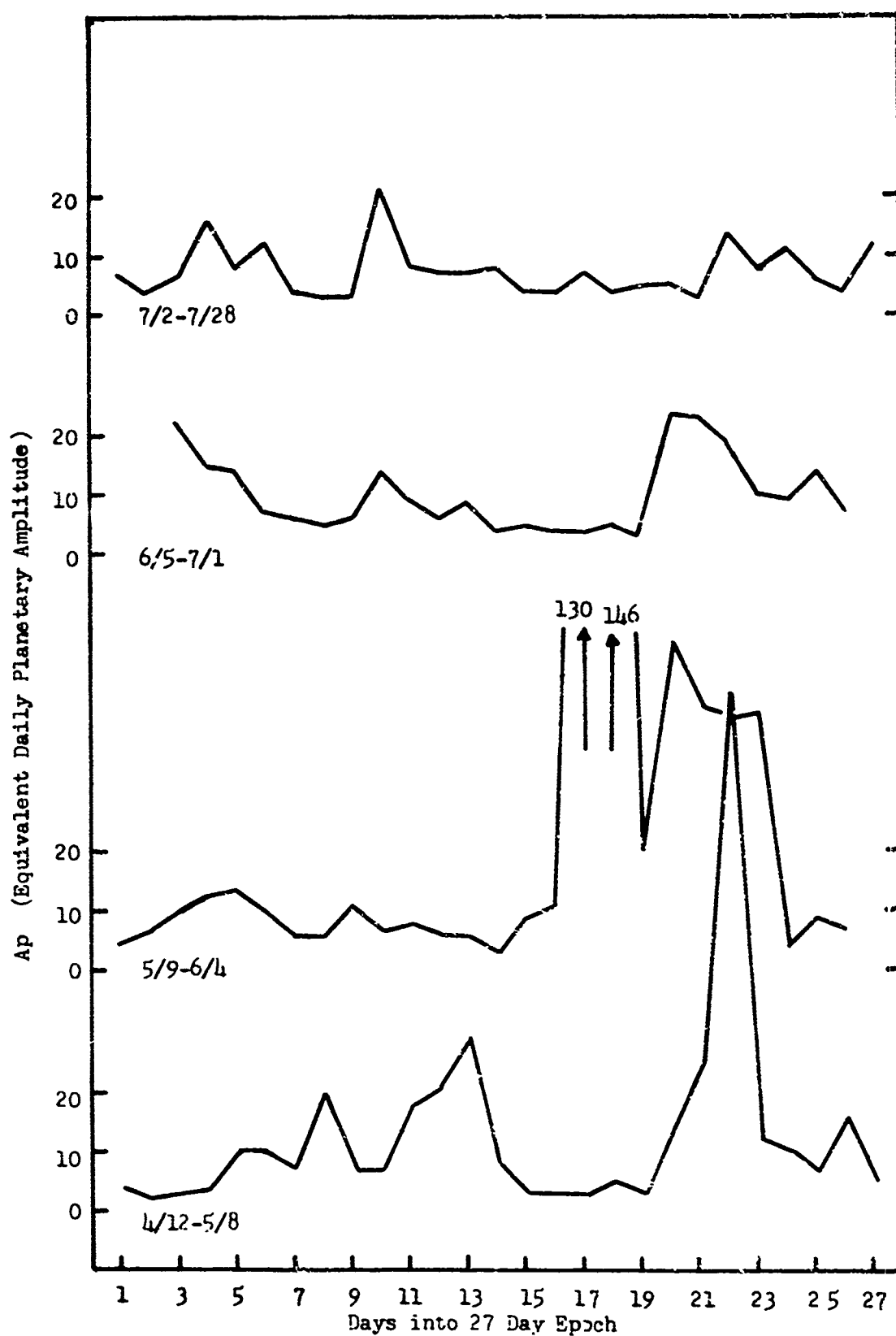Figure 7.

47
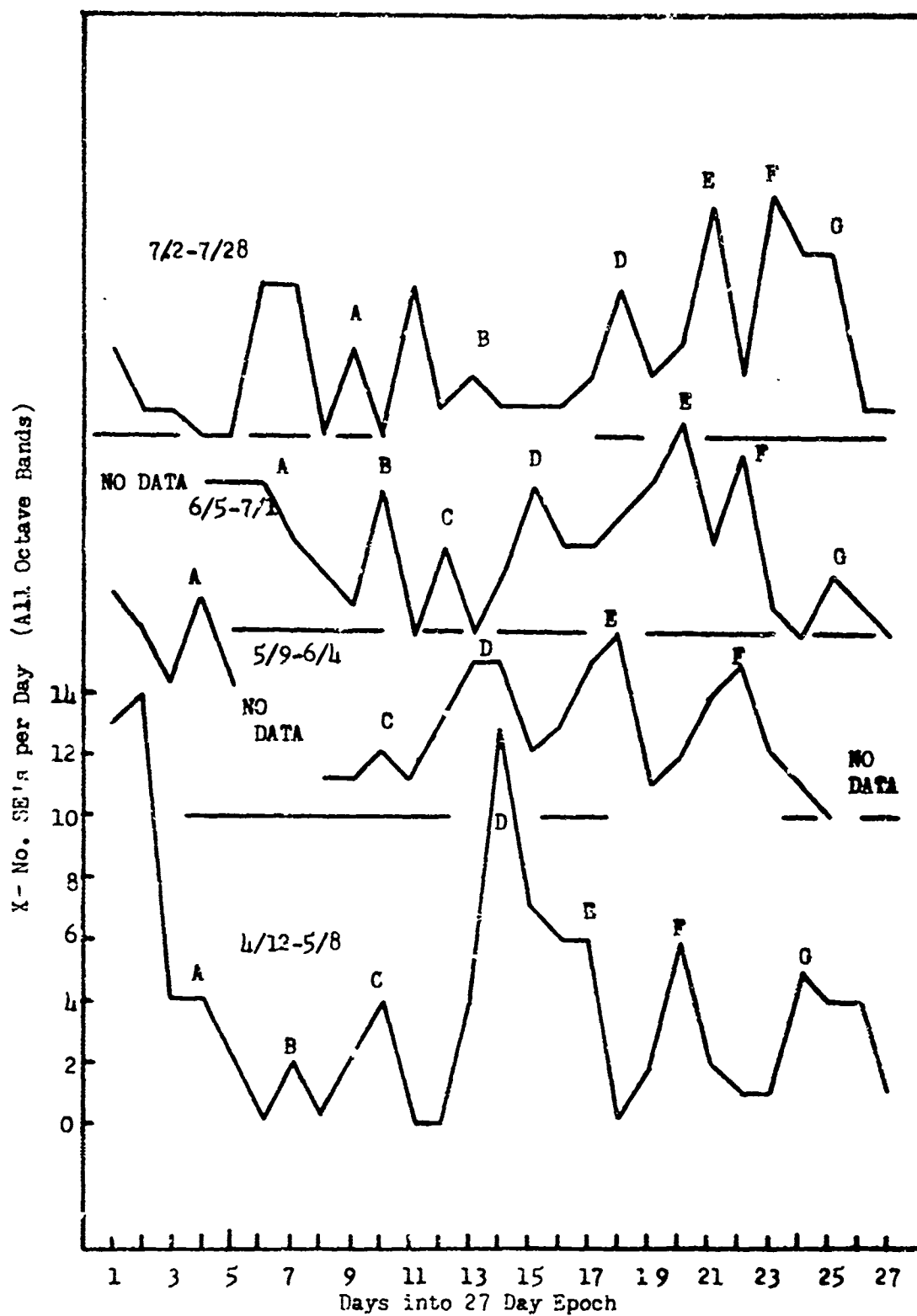
Figure 8.

Figure 9.
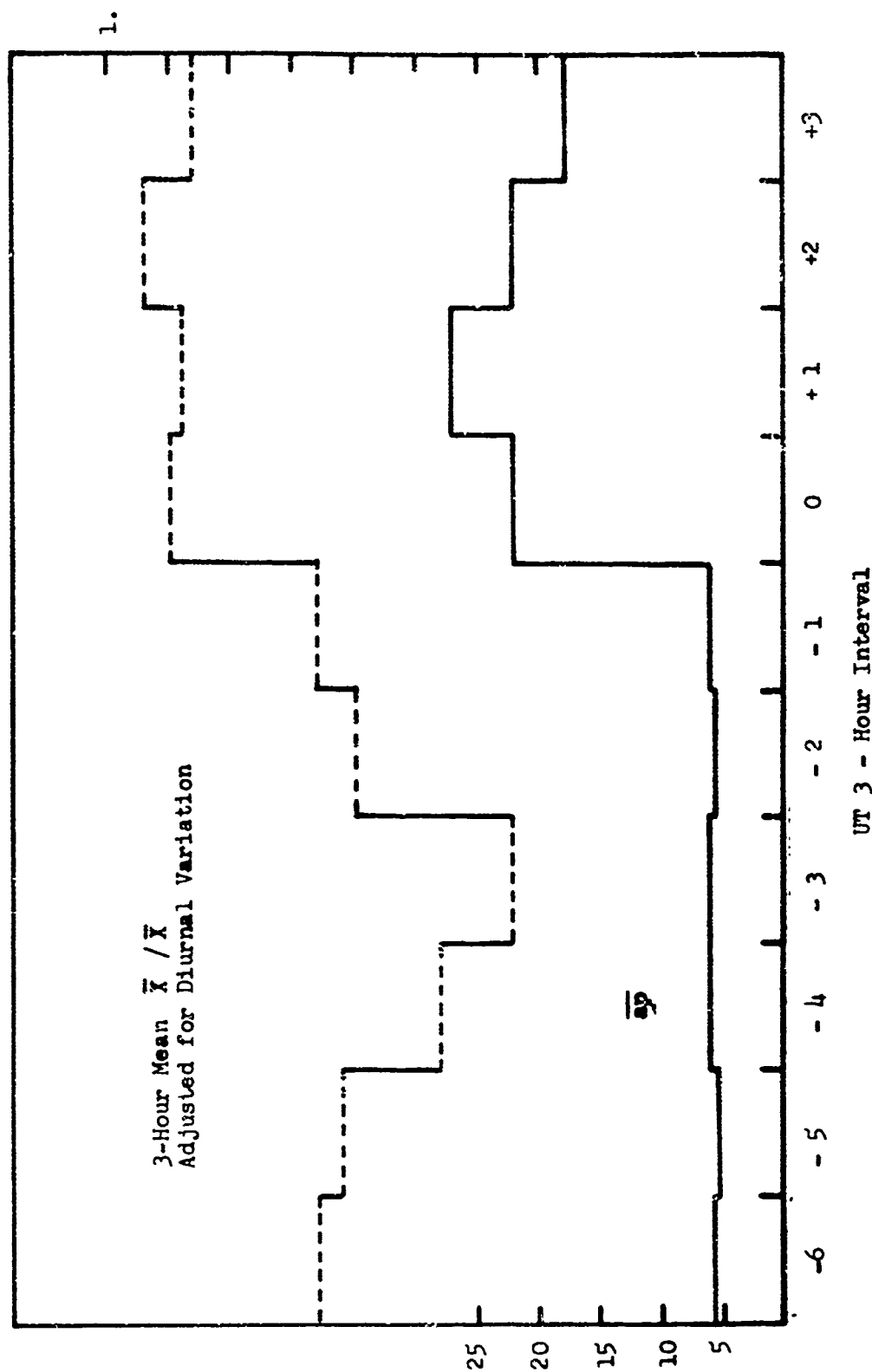
Figure 10.

50

Figure 11.

Figure 12.
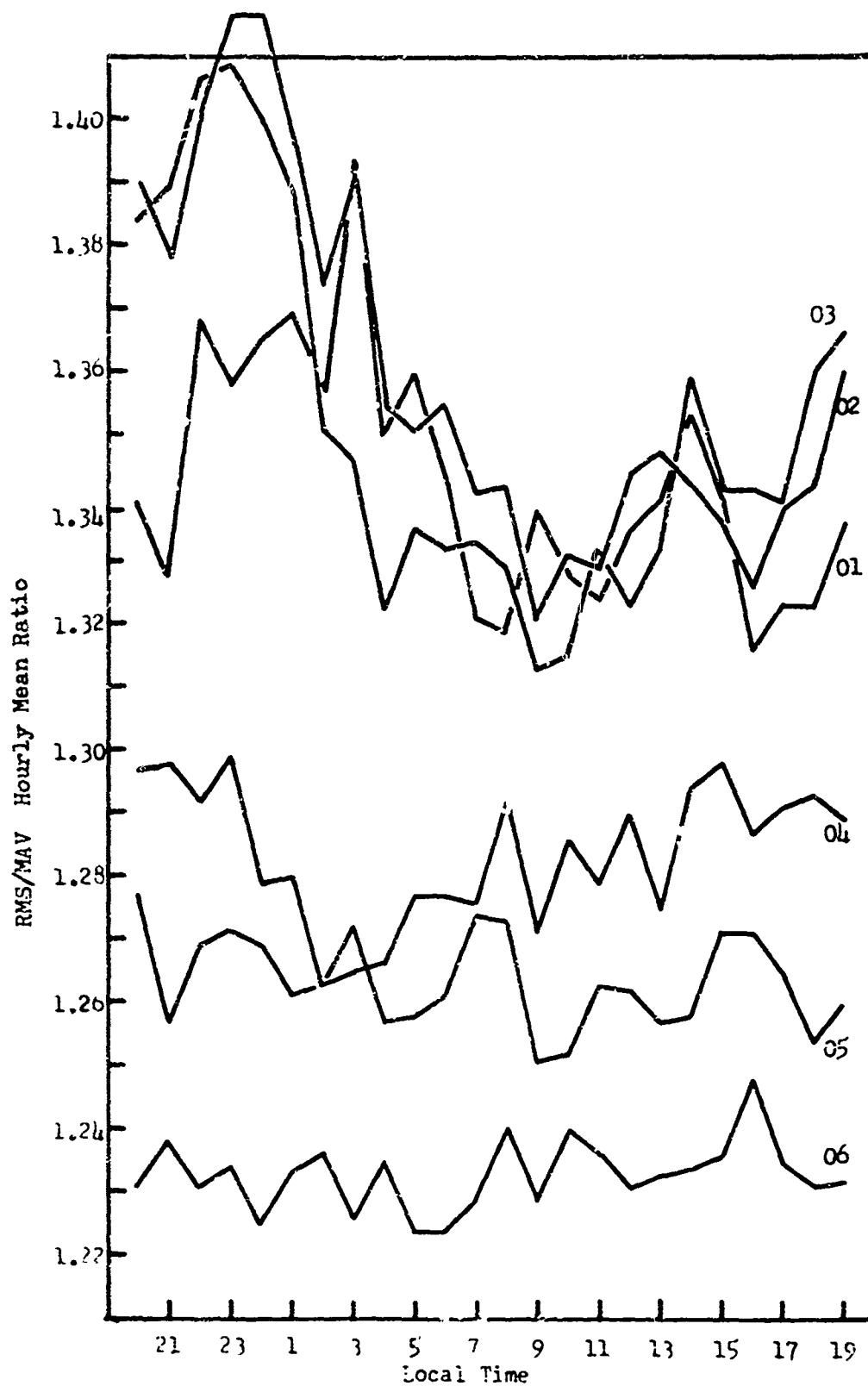
Figure 13.

53

References

Brice, N. M. _J. Geophys. Res._, 72, 5193-5211, 1967.

Carpenter, D. L. _J. Geophys. Res._, 71, 693-709, 1966.

Frey, J. H. _Final Report_, AFCRL-69-0442, 23-29, 1969.

Frey, J. H., W. L. Fischer and D. L. Miller. _Final Report_,
   AFCRL-70-0654, 72 pp., 1970.

Frey, J. H., W. L. Fischer, E. Maple and E. J. Chernosky.
   J. Geomag. and Geoelec., 23, 61-82, 1971.

Hartz, T. R., and N. M. Brice _Planet Space Sci._, 15, 301, 1967.

Nishida, A. _J. Geophys. Res._, 71, 5669-5679, 1966.

Sari, J. W. and N. F. Ness _Preprint, Goddard Space Flight Center_,
   X-616-68-318, 20 pp., 1968.

Silsbee, H. C. and E. H. Vestine _Terr. Mag. and Atmos. Elec._,
   47, 195-208, 1942.

Snyder, C. W., M. Neugebauer and U. R. Rao _J. Geophys. Res._,
   68, 6361-6370, 1963.

Wilson, C. R. _J. Geophys. Res._, 67, 2054-2056, 1962.

Scientists Who Contributed to the Research

John H. Frey, Principal Investigator

William H. Fischer, Senior Research Physicist

55